Volume 16, Issue 4, 162514 (1-14)

International Journal of Industrial Chemistry (IJIC)

https://doi.org/10.57647/j.ijic.2025.1604.14

Chickweed-Derived Natural Surfactant and Nano-TiO_2 for Enhanced Oil Recovery in Carbonate Reservoirs

Saeid Alamdari, Moein Nabipour *, Amin Azdarpour, Bizhan Honarvar, Nadia Esfandiari

Department of Chemical Engineering, Marv. C., Islamic Azad University, Marvdasht, Iran

* **Corresponding authors:** moein.nabipour@iau.ac.ir; nabipour@gmail.com

Research Article:

Received:
23 August 2025

Revised:
30 September 2025

Accepted:
25 December 2025

Published in Issue:
30 December 2025

Abstract

This study investigates the potential of chickweed (CW)–derived natural surfactants, combined with titanium dioxide nanoparticles (Nano-TiO_2), for enhanced oil recovery (EOR) in carbonate reservoirs. The addition of Nano-TiO_2 further improved stability, interfacial tension (IFT) reduction, and wettability alteration, benefiting from synergistic interactions between nanoparticles, surfactant molecules, and divalent cations. Foamability studies revealed strong and persistent foaming behavior, indicating additional potential for mobility control. Core flooding experiments confirmed that tertiary injection of chickweed surfactant increased recovery by approximately 14% original oil in place (OOIP), while the hybrid surfactant–nanoparticle solution achieved approximately 20% OOIP, outperforming surfactant-only flooding. These results demonstrate that chickweed-derived surfactants, especially in combination with nanoparticles, provide an eco-friendly and effective alternative to synthetic chemicals for EOR applications in challenging carbonate reservoirs.

Keywords: Chickweed; EOR; Natural surfactant; Nano-TiO_2; Oil recovery factor

Cite this article: Alamdari S, Nabipour M, Azdarpour A, Honarvar B, Esfandiari N. Chickweed-Derived Natural Surfactant and Nano-TiO_2 for Enhanced Oil Recovery in Carbonate Reservoirs. Int. J. Ind. Chem., 2025; 16(4):1-14. https://doi.org/10.57647/j.ijic.2025.1604.14

1. Introduction

Improving oil recovery from conventional reservoirs remains a major challenge in the petroleum industry, as primary and secondary recovery methods typically extract only a fraction of the original oil in place, leaving a significant amount of hydrocarbons trapped in the reservoir. To address this limitation, EOR techniques have been developed, aiming to mobilize residual oil through various mechanisms such as pressure maintenance, wettability alteration, and IFT reduction [1–4]. Among these techniques, chemical flooding has emerged as an effective EOR approach, where chemicals such as surfactants, polymers, or alkalis are injected to improve sweep efficiency and displace oil that cannot be recovered through conventional methods. Surfactant flooding, in particular, has gained attention due to its ability to simultaneously reduce IFT and modify rock wettability, thereby significantly enhancing the recovery factor [5–10].

In recent years, natural surfactants have attracted interest as environmentally friendly and cost-effective alternatives to synthetic chemicals in EOR applications. These bio-based surfactants offer comparable performance in reducing IFT and altering wettability while minimizing environmental impact [11–18]. Despite growing research on natural surfactant flooding, limited studies have investigated the combined effect of natural surfactants with different salinity solutions under reservoir-relevant conditions, including high temperature.

Sami et al. extracted a novel bio-based surfactant from Avena sativa (AS) and evaluated its performance in the presence of various salts commonly found in seawater. Their study also determined the optimal salinity for

seawater when used with the AS surfactant. The results indicated that the critical micelle concentration (CMC) of the AS surfactant is 4000 ppm. In terms of IFT and contact angle reduction, diluted seawater with a salinity of 2000 ppm was found to be the most effective when combined with the AS surfactant. The lowest IFT measured among the tested salts was 1.38 mN/m, achieved with Na_2CO_3 in combination with the surfactant at its CMC. Following the injection of 5 PVs of this solution, a minimum contact angle of 38.28° was observed, and the tertiary oil recovery factor increased by 28.98% [15].

Moradi et al. (2025) examined the influence of a natural surfactant derived from Tribulus terrestris on oil recovery during smart water flooding. In their study, synthetic seawater with varying concentrations of Ca^{2+}, Mg^{2+}, and SO_4^{2-} ions were employed as smart water. The results demonstrated that the nonionic natural surfactant exhibited excellent compatibility with smart water, effectively enhancing oil recovery in carbonate reservoirs. When the surfactant was used alongside seawater with different active ion concentrations, significant reductions in oil–water interfacial tension (13.5 mN/m) and contact angle (54.4°) were observed. Furthermore, the oil recovery factor increased to 72% under the combined action of smart water and the natural surfactant [19].

In a study conducted by Azdarpour et al. (2023), the synergistic effects of a natural surfactant extracted from alfalfa and smart water, particularly the contributions of Ca^{2+}, Mg^{2+}, and SO_4^{2-} ions, were investigated in carbonate reservoirs. Their experiments demonstrated that the combination of natural surfactant with smart water significantly reduced the interfacial tension by 71% and lowered the contact angle to 63.2°. The study highlighted that Ca^{2+} had a more pronounced effect than Mg^{2+} and SO_4^{2-} in enhancing oil recovery during smart water flooding with the surfactant. Moreover, they identified that a formulation consisting of seawater with triple the normal Ca^{2+} concentration and 4 wt% natural surfactant was the most effective, achieving an oil recovery of 62% [20].

Recent studies have also highlighted the potential of plant-derived surfactants for EOR. For example, Camacho and co-workers extracted an anionic surfactant from Madhuca longifolia (Mahua) oil and evaluated its performance through IFT and contact angle measurements. Their results demonstrated that the Mahua-derived surfactant achieved a CMC of 9000 ppm and, under optimum salinity conditions, reduced the oil–water IFT to an ultralow value of 0.01 mN/m. Wettability tests confirmed a significant alteration of rock surfaces from oil-wet to strongly water-wet, with the contact angle decreasing to as low as 8°. Core flooding experiments further confirmed its effectiveness, with tertiary surfactant injection yielding a maximum oil recovery of 77.92% of the OOIP. These findings reinforce the viability of natural surfactants as green alternatives for chemical EOR, with performance comparable to or exceeding many synthetic counterparts [21].

Although natural surfactants have increasingly been explored as eco-friendly agents for chemical EOR, the available literature remains fragmented in several important aspects. Most existing studies focus on a narrow selection of plant-derived surfactants and typically evaluate them under simplified laboratory conditions, often neglecting the combined influence of reservoir salinity, divalent cations, temperature, and soaking time on interfacial behavior and wettability evolution. Furthermore, only limited attention has been given to coupling natural surfactants with nanoparticles, despite growing evidence that synergistic interactions between the two can substantially improve interfacial stability and wettability alteration in carbonate systems.

A major unresolved gap is the absence of studies involving Stellaria media (chickweed), an unexplored botanical source whose saponin-rich composition may offer interfacial properties comparable to or better than commonly studied natural surfactants. Additionally, most prior EOR investigations overlook long-term fluid compatibility and do not validate their formulations in core-scale displacement tests under reservoir-representative conditions. The present study addresses these shortcomings by introducing chickweed-derived saponins as a new class of natural surfactants and demonstrating, for the first time, their enhanced performance when combined with Nano-TiO_2. By systematically evaluating interfacial tension, wettability progression, foamability, and tertiary-coreflood recovery in high-temperature, high-salinity environments, this work bridges critical knowledge gaps and provides a more realistic and comprehensive assessment of the viability of natural surfactant–nanoparticle systems for carbonate EOR.

2. Materials and Methods

2.1. Materials

Dried chickweed (Stellaria media) was used as the raw material for saponin extraction in this study. Fresh plants were first washed thoroughly to remove soil and surface impurities, then air-dried under shade conditions to preserve thermally sensitive compounds. The dried material was ground into a fine powder using a laboratory mill to increase surface area and improve solvent penetration during extraction. This powdered chickweed served as the feedstock for subsequent ethanol–water solvent extraction of saponins, ensuring consistency and reproducibility of the natural surfactant preparation. In

addition, Nano-TiO_2 was purchased locally and used in this study.A crude oil sample with an API gravity of 31.56° was selected from a reservoir located in southern Iran for use in this investigation. The SARA analysis of the crude sample showed that saturate, aromatic, resin, and asphaltene content of the crude oil is 53.35, 32.28, 9.78, and 4.59 wt%, respectively. In addition, acid number (AN) and base number (BN) of the crude oil was 1.63 and 0.46, respectively. Carbonate core specimens for this research were obtained from outcrop sections of a carbonate reservoir in Iran. Their porosity and permeability were measured through helium porosimeter and brine permeability tests, respectively. The porosity of the samples was 11.26 to 11.33%, while the permeability ranged between 14.87 and 14.98 mD, while their length was 7.59 and 7.62 cm. In addition, according to the XRD analysis, the rock is primarily composed of calcite (50%), followed by dolomite (33%), with the remaining 17% attributed to other mineral constituents. For the experimental section, formation brine with total dissolved solids (TDS) of 97645 ppm was obtained from the same oil field and utilized as the aqueous phase. The methodology of measuring TDS, porosity, permeability and XRD analysis was carefully followed from the literature data [22–26]. Moreover, analytical-grade salts, $MgCl_2$, NaCl, and KCl, were employed to prepare synthetic brine solutions. These salts were sourced locally and had a reported purity of 99%.

2.2. Extraction of saponin from cheekweed

The saponin extraction procedure employed in this work followed the methodology reported in our earlier publications [15]. Briefly, 100 g of dried CW powder was placed in a Soxhlet extractor, and 500 mL of methanol was circulated for approximately 10 hours. The resulting extract was then subjected to rotary evaporation to remove methanol and recover the crude surfactant fraction. The dried residue was subsequently mixed with 50 mL of distilled water in a separatory funnel, after which 50 mL of n-butanol was introduced. The mixture was stirred for nearly 2 hours to facilitate separation of the aqueous and organic phases. The n-butanol fraction containing the desired organic compounds was then isolated and concentrated again using a rotary evaporator.In the next stage, diethyl ether was added to the concentrated extract and the solution was centrifuged at 3500 rpm for about 20 minutes. This process yielded a brown-colored saponin-rich compound. The extraction efficiency of saponin from CW powder under these conditions was determined to be 3.84%.

2.3. Characterization of saponin

To investigate the characteristics of the extracted saponin, a combination of analytical techniques was employed, including ^{1}H NMR and FT-IR. Structural information was obtained through proton nuclear magnetic resonance (^{1}H NMR) by dissolving the natural surfactant in DMSO-d_6 and analyzing the solution with a Bruker 500 MHz spectrometer at 25 °C. Functional groups and bonding environments were identified through Fourier transform infrared (FT-IR) spectroscopy, performed with a VARIAN Inova spectrometer (USA) over the range of 500–4000 cm^{-1}.

2.4. IFT and contact angle measurement

The IFT between various solutions and crude oil under reservoir conditions was measured using the IFT400 apparatus (Fars EOR Tech. Co., Iran). This technique employs the pendant drop method in combination with Axisymmetric Drop Shape Analysis (ADSA) to determine IFT values as explained by previous researchers [15].

The apparatus can operate at pressures up to 6000 psia and temperatures up to 400 °F. In this method, the IFT between the two phases (γ, mN/m) is calculated using Eq. (1), where Δρ represents the density difference between the fluids, g is the gravitational acceleration, D denotes the drop's maximum diameter, and H is the shape factor. Captured drop images are subsequently analyzed with the ADSA technique to obtain the IFT values.

An uncertainty of ±5% was applied when reporting IFT results. In this study, various solutions were prepared, and their IFTs with crude oil were measured at 80 °C.

$$\gamma = \frac{\Delta\rho g D^2}{H} \qquad (1)$$

The effect of various solutions on rock wettability was assessed using the contact angle method. Contact angle measurements were performed with the IFT400 instrument.

Rock slices were first saturated with oil for 40 days at 80 °C to alter their wettability from water-wet to oil-wet. Subsequently, the sessile drop method was employed, and the contact angle of an oil droplet was measured in the presence of different solutions at 80 °C and atmospheric pressure.

Measurements were taken over time intervals up to 195 hours. Each experiment was conducted in triplicate, and the median value was reported to minimize experimental errors. Additionally, both the left and right contact angles of each droplet were recorded, and the average of these values was reported for each test [27–29].

2.5. Oil recovery factor measurement

In this study, a core flooding apparatus (Fars EOR Co., Iran) was used to measure oil recovery. The setup consisted of three 500 mL fluid accumulators, a stainless-steel core holder, an HPLC pump, a hand-operated pump for confining pressure, a gas back-pressure regulator rated at 400 bar, an oven for temperature control, and a differential pressure measurement device. Throughout all experiments, both the produced oil volume and pressure differentials were continuously recorded for analysis. The core flooding procedure, as described by previous researchers [5,30,31], was followed closely. It is worth mentioning that the procedure explained by previous researchers was followed carefully for obtaining connate water saturation. First, the core samples were cleaned with toluene and acetone. After cleaning, they were dried overnight at 70 °C, and their weights were monitored before and after drying. Each core was then placed in a saturator, evacuated under vacuum for one hour, and subsequently saturated with formation brine under 3500 psi for 24 hours. The saturated cores were positioned in the core holder, where 5 PV of formation brine was injected at 80 °C and 4500 psi to establish equilibrium. Next, about 5 PV of dead oil was injected under the same conditions to achieve residual water saturation. To restore original wettability and equilibrate the rock–brine–oil system, the cores were aged in crude oil at 80 °C for approximately one month. Secondary recovery was then carried out by injecting 5 PV of formation brine at 80 °C and 4500 psi. Tertiary recovery followed, using 5 PV of a solution containing 4000 ppm natural surfactant and FB at a flow rate of 0.3 cc/min, injected in two stages: an initial 3 PV, followed by a 135-hour soaking period, and then the remaining 2 PV, with the soaking time selected based on contact angle measurements. Finally, the same tertiary procedure was repeated using 4000 ppm natural surfactant in FB (LoSal solution) combined with 2000 ppm Nano-TiO_2.

3. Results and Discussions

3.1. Characterization of natural surfactant extracted from

The FT-IR spectrum of the chickweed-derived natural surfactant as shown in Figure 1(a) provides crucial insights into the molecular composition of the extract and validates the successful isolation of saponin-like compounds, which are responsible for its surface-active properties.

The broad absorption band observed around 3400 cm^{-1} is indicative of O–H stretching vibrations, confirming the presence of hydroxyl groups.

These groups are expected in glycosidic linkages and sugar moieties, which are characteristic features of plant-derived saponins. Hydroxyl groups are critical for hydrogen bonding with water molecules, enhancing solubility and interfacial activity under reservoir conditions. Distinct peaks between 2920 and 2850 cm^{-1} are attributed to asymmetric and symmetric C–H stretching vibrations of aliphatic $–CH_2$ and $–CH_3$ groups. The intensity of these peaks reflects the abundance of hydrophobic alkyl chains within the extract. These hydrocarbon tails provide the hydrophobic component of the amphiphilic structure, which is essential for adsorption at oil–water interfaces and the subsequent reduction of interfacial tension (IFT).

This amphiphilic nature is the key to the surfactant's function in enhanced oil recovery (EOR) applications. Another strong absorption band is observed at ~1650 cm^{-1}, which is characteristic of C=C stretching vibrations in unsaturated bonds or carbonyl groups (C=O) associated with triterpenoid structures. The presence of unsaturation within the aglycone portion of the molecule is a hallmark of many saponins and may contribute to molecular flexibility and improved interfacial packing at the crude oil–water boundary. Additionally, bands around 1450 cm^{-1} correspond to bending vibrations of $–CH_2$ groups, further emphasizing the contribution of aliphatic moieties to the surfactant framework. In the fingerprint region, strong absorptions are detected between 1050 and 1150 cm^{-1}, which correspond to C–O–C and C–O stretching vibrations of ether and glycosidic linkages.

These peaks strongly support the glycosidic nature of the extract, confirming that the surfactant is indeed composed of sugar conjugates bound to a triterpenoid backbone. The vibrational signature at ~890 cm^{-1} further indicates the presence of glycosidic bonds in β-anomeric configuration, which is consistent with the molecular structure of saponins reported in earlier phytochemical studies.

Overall, the FT-IR spectrum demonstrates that the chickweed extract possesses the defining features of a natural surfactant: hydrophilic sugar residues and hydrophobic hydrocarbon backbones. This dual chemical character is essential for adsorption at oil–water interfaces and contributes directly to IFT reduction and wettability modification. Compared with literature reports on saponins extracted from Sapindus mukorossi (soapnut) and Quillaja saponaria, the chickweed-derived extract exhibits similar spectral features, suggesting comparable surface activity.

Therefore, the FT-IR evidence not only validates the extraction procedure but also supports the potential application of chickweed as a sustainable, plant-based source of natural surfactants for EOR operations [15,18,20].

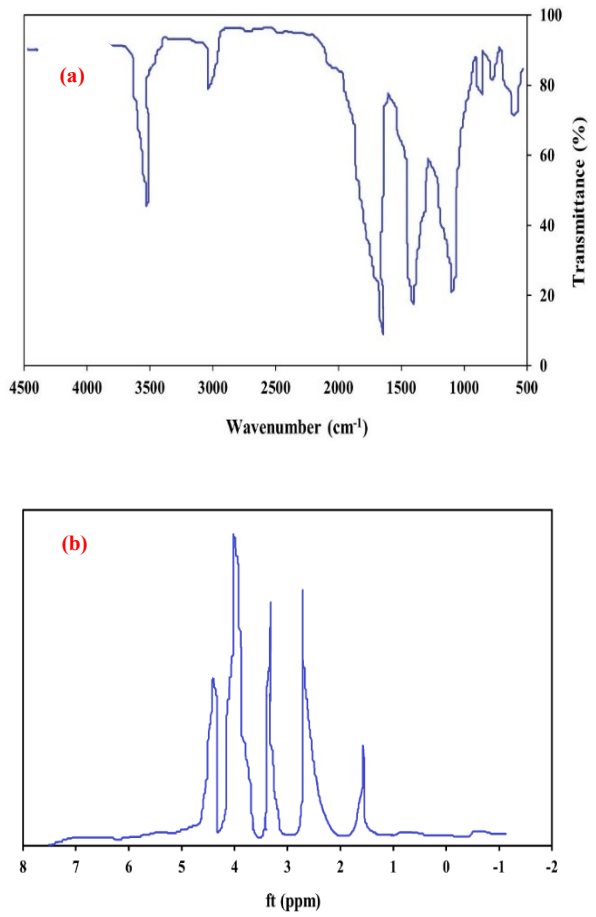

Figure 1. (a). FT-IR curve of natural surfactant extracted from CW; (b): HNMR curve of natural surfactant extracted from CW

The ^{1}H-NMR spectrum of the natural surfactant extracted from chickweed as shown in Figure 1(b) provides direct structural confirmation of the molecular constituents inferred from the FT-IR analysis. The spectrum displays multiple chemical shifts that can be correlated to both hydrophobic and hydrophilic domains of saponin-like molecules, further validating their amphiphilic nature. In the upfield region (δ 0.8–1.2 ppm), strong singlets and doublets are observed, which correspond to terminal methyl protons (–CH_3) attached to aliphatic chains. The relative intensity of these signals indicates that the extract contains a significant proportion of long hydrocarbon moieties, consistent with triterpenoid or steroidal backbones commonly reported for saponins. These aliphatic signals provide evidence for the hydrophobic segment of the molecule, which drives adsorption at oil–water interfaces. Between δ 1.2 and 2.0 ppm, multiplets are detected, representing methylene (–CH_2–) protons of aliphatic chains.

These protons contribute to the flexibility of the molecular backbone, enabling conformational adjustments that facilitate close packing of surfactant molecules at the crude oil–water boundary. The presence of well-defined methylene signals suggests that the surfactant molecules possess relatively long hydrocarbon tails, which is a desirable property for efficient IFT reduction in EOR applications. In the downfield region, peaks between δ 3.0 and 4.5 ppm are clearly visible, corresponding to protons attached to carbons bearing hydroxyl or glycosidic groups.

These signals are diagnostic of sugar residues, which form the hydrophilic headgroups of the surfactant. The multiplicity of these resonances indicates a complex mixture of protons associated with different sugar moieties, consistent with the natural diversity of saponins extracted from plant material. Importantly, these hydrophilic segments contribute to the solubility of the surfactant in aqueous phases, ensuring stability under reservoir conditions.

Another critical feature is the resonance observed between δ 5.0 and 5.5 ppm, which is assigned to anomeric protons of glycosidic linkages. This downfield shift confirms the presence of sugar units covalently bound to the aglycone backbone, a structural hallmark of saponins. The intensity of the anomeric proton peaks provides strong evidence of glycosidic substitution, which enhances hydrophilicity and is essential for foam stabilization and wettability alteration in EOR processes [32–34]. The combined spectral features validate that the chickweed-derived extract contains amphiphilic molecules structurally consistent with natural saponins: hydrophobic triterpenoid backbones conjugated with hydrophilic sugar moieties. This duality explains the surfactant's observed ability to lower IFT and modify wettability in subsequent experimental evaluations. Comparisons with published NMR spectra of Sapindus mukorossi and Quillaja saponaria extracts show similar chemical shift patterns, suggesting that chickweed may serve as a comparable, yet underexplored, natural surfactant source. The confirmation of glycosidic structures through NMR significantly strengthens the evidence that chickweed-derived surfactants are viable candidates for EOR applications, combining environmental sustainability with practical interfacial activity [32–34].

3.2. Compatibility of fluids

Figure 2 shows that, over a 30-day ageing period at 80 °C, solutions containing the chickweed-derived surfactant (at the test concentration) and those containing surfactant + 2000 ppm Nano-TiO_2 remain visually homogeneous with no macroscopic phase separation, flocculation, or visible precipitation. There is no evidence of turbidity increase beyond early, mild baseline scattering, and no solid sediment collects at the bottom of the test vials. The nanoparticle suspension retains a uniform appearance comparable to the freshly prepared state. The long-term visual stability in high-temperature brine indicates two

complementary stabilizing mechanisms. First, the chickweed saponins provide steric and electrostatic stabilization to dispersed phases through hydrophilic sugar headgroups that hydrate strongly and form solvation shells; these slow aggregation of hydrophobic domains and screen bridging by divalent cations. Second, Nano-TiO_2 particles often carry surface hydroxyl groups that can hydrogen-bond with surfactant headgroups and adsorb a surfactant layer. This adsorbed layer both changes the surface charge distribution of the particles and produces steric hindrance that prevents aggregation even in the presence of high ionic strength and divalent cations. At 80 °C, increased Brownian motion and weakened double layers could promote aggregation, but the combination of hydration (from glycosides) and steric barriers (from adsorbed surfactant) compensates for electrostatic compression, maintaining dispersion.

Other studies of natural saponin-based surfactants show similar compatibility windows when proper extraction/purification preserves hydrophilic sugar moieties; for example, saponins from Quillaja or Sapindus have been reported to stabilize nanoparticles and resist salting out up to moderate brine salinities when the surfactant concentration exceeds the CMC and when nanoparticles are precoated. The observed stability here is consistent with those findings, though each plant extract has a specific tolerance depending on headgroup chemistry and tail length. Compatibility over 30 days at 80 °C suggests the formulation is suitable for injection and short-to-mid-term reservoir residence. Practically, this reduces the risk of pore blockage by precipitates or nanoparticle aggregation during tertiary recovery operations. It also implies the surfactant–nanoparticle hybrid can reach deeper zones without early loss of activity, enabling the advantages of both IFT reduction and nanoparticle-mediated interfacial stabilization in the reservoir [35,36].

3.3. CMC of natural surfactant

Figure 3 shows IFT between crude oil and aqueous phases containing the chickweed surfactant versus temperature. The baseline oil–DIW IFT is high (typical of unmodified crude), and adding the surfactant markedly reduces IFT at all measured temperatures. The reduction is concentration-dependent (stronger at/above CMC) and becomes more pronounced as temperature increases from ambient up to reservoir temperatures (e.g., approaching 80 °C): the IFT curve slopes downward with temperature, indicating lower IFT at higher temperatures for the same surfactant concentration. Three interrelated mechanisms drive the observed temperature dependence. (1) Kinetics: higher temperature increases molecular diffusion and lowers viscosity, accelerating surfactant transport to the oil–water interface and enhancing adsorption rates. (2) Thermodynamics: higher thermal energy reduces the free energy penalty for interfacial adsorption and encourages surfactant packing, which lowers interfacial tension. (3) Crude oil composition: elevated temperature can partially solubilize or mobilize heavy polar components (asphaltenes, resins), allowing surfactant molecules to interact more effectively with the oil phase and displace strongly-bound surface active components.

The chickweed saponins' sugar headgroups likely remain hydrated and surface-active at elevated temperatures, while the hydrocarbon tails increase interfacial anchoring, collectively resulting in greater IFT reduction at higher temperatures [37,38]. Temperature-enhanced interfacial activity is common among natural saponins and synthetic surfactants; however, some surfactants suffer thermal degradation or reduced hydration at high temperatures.

Figure 2. Compatibility of natural surfactant and Nano-TiO2 with FB at 80 ℃ after 30 days for visualizing possible precipitation due the interactions of fluids

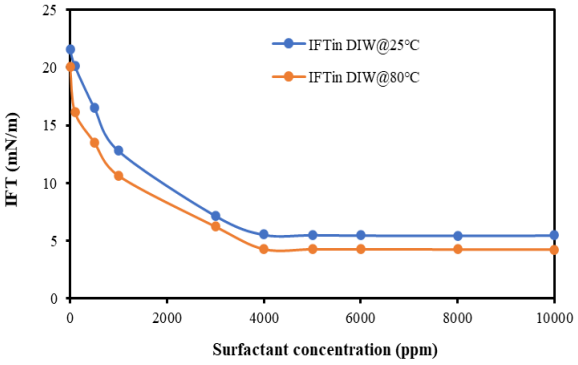

Figure 3. IFT values of natural surfactant with crude oil and DIW at different temperatures for measuring CMC value of natural surfactant

The figure suggests chickweed extract retains activity under the tested range, comparable to other robust natural saponins reported in EOR literature. Where differences arise, they are often due to tail length (longer tails favor lower IFT but may be more temperature-sensitive) and headgroup polarity. Lower IFT at reservoir temperatures improves capillary-pressure reduction and increases the likelihood of mobilizing trapped oil. The enhanced performance at elevated temperature implies the extract is suited for moderately high-temperature carbonate reservoirs; practitioners can expect greater performance in situ vs. lab ambient measurements. For field design, this supports applying the surfactant in warmer zones or pre-heating where feasible to maximize displacement efficiency [39,40].

3.4. Foamability of natural surfactant

Figure 4 reports foam height versus time (or foamability vs. time) when DIW is sparged through solution containing the chickweed surfactant. The surfactant forms a high initial foam volume soon after gas sparging; foam collapse is slow, with a significant residual foam height even after tens of minutes. The time-decay curve shows an initial fast drainage phase followed by a much slower coalescence/decay phase, typical of stable foams.

Foam formation and stability are controlled by surfactant adsorption kinetics, surface rheology, and film elasticity. The saponin glycosides form viscoelastic surface films: sugar headgroups create hydrogen-bonded networks and promote hydration, while rigid triterpenoid backbones provide mechanical strength to the film, resisting rupture. The result is lower film drainage and slower coalescence. Additionally, the extract may generate a high surface modulus (resistance to deformation), reducing Marangoni flows that otherwise thin films and destabilize foam. If minor impurities like natural polysaccharides are present, they can further increase bulk viscosity and slow drainage, enhancing foam life.

Saponin foams (e.g., from Quillaja or Sapindus) are widely reported to be more stable than many synthetic surfactant foams at similar concentrations, due to the rigid interfacial films described above. The chickweed foam behavior mirrors these observations, suggesting its suitability where foam is required for mobility control. High foamability and stability are beneficial for gas-foam EOR and mobility control: foam reduces gas mobility, mitigates early breakthrough, and improves sweep efficiency in heterogeneous formations [41,42]. For field implementation, the ability to sustain foam over operationally relevant timescales means fewer injections may achieve desired conformance, provided foam propagation and resistance factors are acceptable in corefloods and field trials [41,42].

3.5. IFT of natural surfactant with crude oil using different solutions

Table 1 shows the sensitivity of IFT to formation brine concentration (which is composed of various ions): IFT decreases from 21.80 mN/m in DIW to a minimum around 12.41 mN/m at 10,000 ppm FB, then modestly increases at higher FB concentrations (e.g., 13.35–14.81 mN/m at 50,000–97,000 ppm). This matches the salt-dependent behavior visible in Figure 9: moderate salinity enhances interfacial action, but excessive salinity begins to reduce effectiveness. Figure 5(a) compares IFT measured at 80 °C for 4000 ppm surfactant solutions containing varying concentrations of $MgCl_2$, NaCl, and KCl. The trend shows that all salts influence IFT relative to pure formation brine, but $MgCl_2$ (divalent) yields the largest IFT reduction at moderate concentrations. Monovalent salts (NaCl, KCl) also lower IFT but to a lesser and more gradual extent. At very high salt concentrations, the rate of IFT decrease slows or slightly reverses, indicative of salting-out or decreased surfactant solubility [43,44]. Ionic strength and ion valence affect surfactant behavior via electrostatic screening and headgroup packing. Divalent cations like Mg^{2+} more effectively compress the electrical double layer of ionic/polar headgroups and can form specific ion pairs or bridging interactions between negatively charged or polar groups on the surfactant and oil constituents. This screening reduces repulsion among headgroups and allows denser packing at the interface, which lowers IFT. For monovalent ions, the screening effect is weaker, so the interfacial packing improvement is smaller.

Figure 4. Foamability of natural surfactant with DIW at ambient temperatures using CMC value of natural surfactant

Table 1. IFT values of 4000 ppm of natural surfactant and crude oil with different concentrations of FB at 80 °C and reservoir pressure

Formation brine concentration (ppm)	IFT (mN/m)
0	21.80
1000	17.09
5000	14.29
10000	12.41
20000	12.86
50000	13.35
75000	13.82
97000	14.81

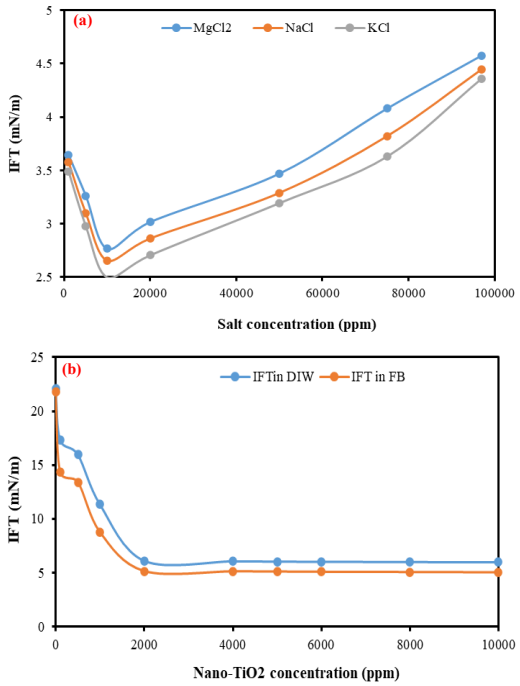

Figure 5. (a): IFT values of 4000 ppm of natural surfactant and crude oil with different concentrations of $MgCl_2$, NaCl, and KCl at 80 °C; (b): IFT values of crude oil with different concentrations of Nano-TiO2 and DIW and FB at 80 °C

However, at very high salinities, surfactant solubility decreases (salting-out), leading to less available surfactant for interfacial adsorption, which explains the plateau or slight increase in IFT at extreme ionic strengths [15,18,20].

The practical takeaway is that the surfactant performs best in moderate salinity environments, and Mg^{2+}-bearing formation waters can actually enhance IFT reduction. For carbonate reservoirs (often high in divalent cations), this is advantageous; however, field formulators should avoid simple upscaling of concentration without checking for salting-out and adsorption losses at very high TDS levels [15,18,20].

Figure 5 (b) shows IFT values as Nano-TiO_2 concentration varies in DIW and in formation brine (FB) at 80 °C. IFT decreases with the addition of nanoparticles up to an optimum concentration (reported in the manuscript as 2000 ppm). Beyond this optimum, further increases produce diminishing returns or slight increases in IFT. The IFT lowering is more pronounced in FB than in DIW at the same nanoparticle concentration, indicating a synergy between nanoparticles and ionic environment. Nanoparticles at the oil–water interface can act as Pickering stabilizers; partially wetted TiO_2 particles adsorb irreversibly to interfaces and lower interfacial energy by replacing higher-energy fluid–fluid contact with lower-energy solid–fluid contacts.

In addition, nanoparticles provide sites for surfactant adsorption and can reorganize interfacial films, lowering IFT. However, excess nanoparticles can aggregate (especially in DIW where screening is limited), reducing available interfacial area and even increasing effective interfacial rigidity, which may impede surfactant packing and cause the observed plateau or slight IFT rise. In formation brine, ionic screening reduces electrostatic repulsion among nanoparticles, allowing better particle packing at the interface and stronger synergy, hence larger IFT reductions at moderate nanoparticle loadings [37,44].

Several studies report an optimum nanoparticle concentration for IFT and emulsion stabilization; too few particles yield weak effects and too many lead to aggregation or pore-blocking risk. The trend seen here aligns with those reports, with TiO_2 proving effective at moderate loadings and showing enhanced interfacial effects in saline media. The identification of an optimum Nano-TiO_2 concentration (e.g., 2000 ppm) is important for designing hybrid surfactant-nanoparticle floods: it balances interfacial benefits against cost and aggregation/pore-blocking risk. In brine-rich carbonate reservoirs, nanoparticle inclusion can be beneficial, but careful screening and dispersion protocols are necessary to avoid formation damage [29,45].

Figure 6 compares IFT for hybrid formulations (surfactant + Nano-TiO_2) across solutions containing NaCl, KCl, and $MgCl_2$ at various concentrations. The hybrid system attains lower IFTs than surfactant-only or nanoparticle-only systems across the board. $MgCl_2$-containing solutions produce the lowest IFTs, followed by NaCl and KCl. The curve shapes echo those in Figure 9: an initial decline in IFT with increasing salt concentration, reaching a minimum in the moderate salinity range, then marginal reversal at very high salinities. Synergism arises because surfactant molecules and nanoparticles operate through complementary mechanisms.

Surfactant reduces IFT by lowering interfacial free energy via adsorption, while nanoparticles provide irreversible interfacial anchoring and steric stabilization. Salts (particularly divalent ions) screen electrostatic repulsion and can bridge polar groups on surfactant headgroups and on nanoparticle surfaces, promoting closer packing and more stable interfacial films. Mg^{2+} acts

as a bridge between negatively polarized oxygens on surfactant sugars and hydroxylated TiO_2 surfaces, increasing interfacial coverage and compactness, thereby lowering IFT more effectively than monovalent cations.

Hybrid surfactant–nanoparticle systems often outperform single-agent formulations, especially in saline conditions. The ordering $Mg^{2+} > Na^+/K^+$ for enhancement is reported in systems where ion bridging is significant and where nanoparticles possess surface hydroxyl groups capable of cation coordination.

The hybrid formulation is promising for field application in carbonate formations with Mg-rich brines. Operators should, however, optimize salt composition and nanoparticle concentration to maintain synergistic effects and minimize colloidal instability or formation plugging risks at high TDS [18,29].

3.6. Contact angle of carbonate rock sample with natural surfactant

Figure 7 presents contact angle measurements on carbonate substrates aged with crude oil under three fluid conditions. In formation brine alone (oil–rock–brine system), the contact angle is high (oil-wet posture). Upon exposure to 4000 ppm chickweed surfactant in FB, the contact angle reduces substantially (indicating a shift toward intermediate or mixed wettability). Adding Nano-TiO_2 to the surfactant solution further reduces the contact angle, moving the system closer to water-wet conditions. Wettability alteration results from competitive adsorption at the rock–oil–brine interface.

The surfactant adsorbs at the rock surface and the oil–water interface, replacing adsorbed crude polar components (resins/asphaltenes) with hydrophilic surfactant headgroups. This lowers the solid–oil interfacial energy and increases the solid–water affinity, hence the reduced contact angle. Nanoparticles amplify this effect via two mechanisms:

(1) they can form a nanoparticle-rich layer at the mineral surface or within the wedge film that physically disrupts oil adhesion;

(2) they promote more robust surfactant adsorption by providing additional adsorption sites and by reducing desorption through mechanical anchoring. The combined result is more effective detachment of oil films and a larger shift toward water-wetness [22,46]. Natural-surfactant-induced wettability alteration has been observed in carbonate systems with many saponins; however, the magnitude of change depends on initial oil wetting and rock mineralogy. The additive effect of nanoparticles is consistent with studies showing nanoparticles facilitate film rupture and surfactant retention at the rock surface. What distinguishes this work is the demonstration of such a synergistic effect using a chickweed extract, which is not widely reported.

Achieving wettability change from strongly oil-wet to intermediate/water-wet significantly improves spontaneous imbibition and displacement efficiency in carbonate rocks, which often suffer from oil-wet tendencies. The hybrid treatment (surfactant + nanoparticles) appears to offer the largest improvement and is thus the preferred tertiary flooding candidate for restoring water-wet conditions and recovering residual oil [35,47].

Figure 8(a) compares contact angles measured after exposure to 4000 ppm surfactant solutions prepared with NaCl, KCl, and $MgCl_2$ at different concentrations. The presence of salts modifies the extent of wettability alteration: $MgCl_2$ produces the largest decrease in contact angle at comparable molarities, while NaCl and KCl produce smaller but still meaningful reductions. Extremely high salt concentrations cause a plateau or mild decrease in the effectiveness of wettability change. Divalent cations (Mg^{2+}) facilitate stronger interactions between surfactant headgroups and carbonate surfaces by forming ionic bridges.

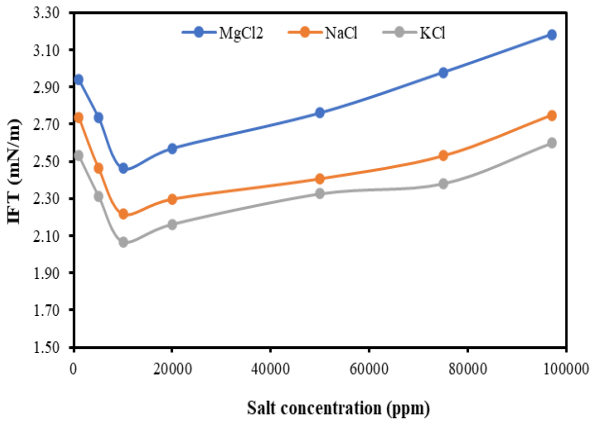

Figure 6. IFT values of crude oil and different solutions prepared by 4000 ppm of natural surfactant and 2000 ppm of nano-TiO_2 with different salts at 80 °C

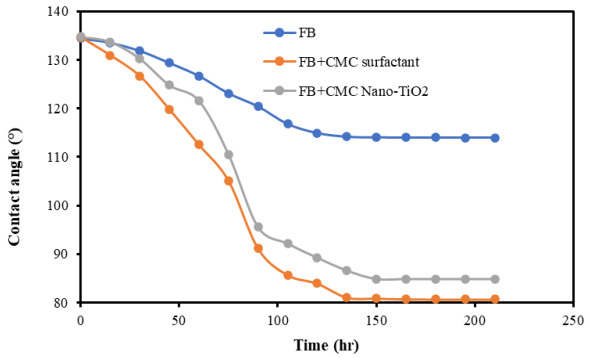

Figure 7. Contact angle of carbonate rock samples with crude oil in the presence of FB, FB and 4000 ppm of natural surfactant, FB, 4000 ppm of natural surfactant and 2000 ppm of Nano-TiO_2

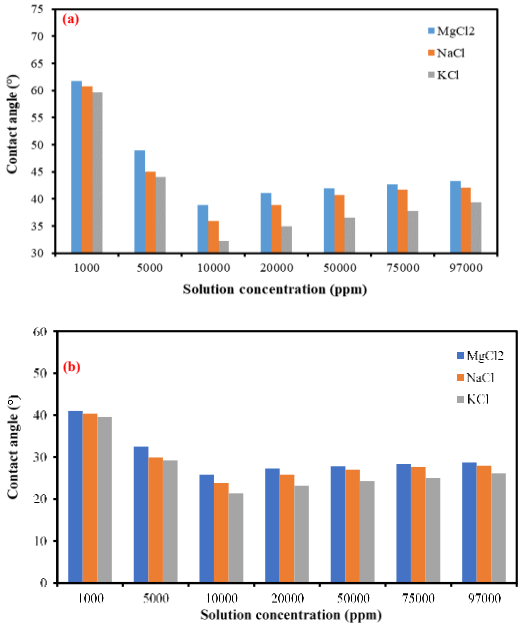

Figure 8. (a): Contact angle of carbonate rock samples with crude oil in the presence 4000 ppm of natural surfactant and different salts; (b): Contact angle of carbonate rock samples with crude oil in the presence 4000 ppm of natural surfactant and 2000 ppm of Nano-TiO_2 and different salts

Carbonate minerals bear surface carbonate and hydroxyl groups capable of complexing with divalent cations; when Mg^{2+} is present, surfactant headgroups (rich in oxygens from glycosidic and hydroxyl groups) can coordinate through cation bridging, creating a strongly adsorbed layer that favors water affinity. Monovalent ions lack the same bridging capability, leading to weaker surfactant-rock anchoring and less pronounced wettability change. At very high salinities, however, competitive adsorption of cations and ionic strength effects reduce surfactant hydration and mobility, tempering the wettability shift.The role of divalent cations in enhancing wettability alteration by surfactants is established in carbonate EOR literature; many studies recommend considering formation cation chemistry when designing chemical floods. The results here are consistent with those observations and provide experimental confirmation for chickweed surfactant. For reservoirs with Mg-rich brines, the chickweed surfactant should be particularly effective at changing wettability favorably. However, formulators must ensure that salinity remains in the window where surfactant hydration and mobility are maintained [35,48].

Figure 8(b) demonstrates the combined influence of salts and nanoparticles on contact angle. Across all salts tested, the surfactant + Nano-TiO_2 formulation gives larger reductions in contact angle than surfactant alone (Figure 8(a)). The best performance is again with $MgCl_2$, where contact angle shifts most dramatically toward water-wet values. NaCl and KCl also benefit from nanoparticle addition, but to lesser extents. Nanoparticles and salts act synergistically: salts screen electrostatic repulsion and enable tighter packing and anchoring of both nanoparticles and surfactant molecules at the rock surface. Divalent cations further create ionic bridges enabling a dense, robust interfacial film containing both surfactant and nanoparticle elements. The nanoparticles act as mechanical wedges that pry oil from the mineral surface and support a structured, persistent hydrophilic film, this combination causes larger and more permanent wettability alteration. Additionally, nanoparticle adsorption reduces surfactant desorption under flow, sustaining alteration under dynamic conditions [25,44].

Hybrid approaches (surfactant + nanoparticles) often show improved wettability alteration over single agents. The observed ranking of salts is consistent with the ionic bridging hypothesis documented in earlier nanoparticle-assisted wettability studies. The hybrid formulation widens the operational window for wettability alteration in carbonate reservoirs and is particularly promising in Mg-rich environments. This suggests that field designs that incorporate nanoparticles will achieve more durable wettability change and therefore better tertiary recovery [48–50].

3.7. Oil recovery factor measurements

Figure 9 summarizes coreflood oil recovery performance when the two tertiary solutions are injected after primary/secondary stages. The surfactant-only tertiary injection produces a measurable incremental oil recovery over baseline water flooding (as reported in your text: ~14% OOIP in earlier summary). The hybrid surfactant + Nano-TiO_2 tertiary injection yields a larger incremental recovery (reported earlier: ~20% OOIP), demonstrating clear enhancement from nanoparticle addition. The production curves show faster and greater oil mobilization for the hybrid solution, with higher cumulative oil and a more sustained production rate during tertiary flooding.
Multiple mechanisms combine to produce the observed recovery improvement:

(1) IFT reduction, surfactant lowers capillary forces, making trapped ganglia mobilizable; (2) wettability alteration, surfactant and nanoparticles shift rock toward water-wet, favoring spontaneous imbibition and increased relative permeability to water; (3) foam and mobility control, the surfactant's foamability (especially where gas is present or generated) can reduce gas mobility and increase sweep; (4) nanoparticle-stabilized emulsions/nanoemulsions, particles promote stable emulsions that aid in carrying mobilized oil to the producer; (5) reduced interfacial film strength, nanoparticles disrupt asphaltene/resin films and anchor surfactant layers that resist desorption.

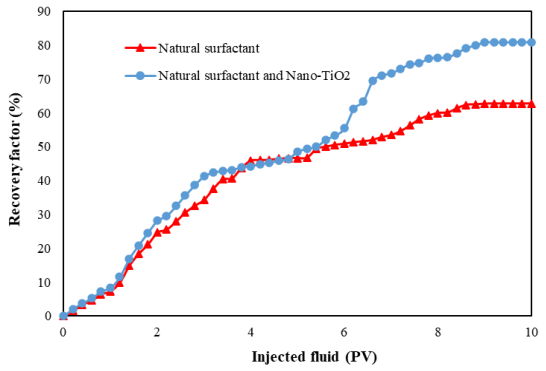

Figure 9. Oil recovery factor with two different solutions as the tertiary recovery, one solution as 4000 ppm of natural surfactant prepared in FB, one solution as 4000 ppm of natural surfactant and 2000 ppm of Nano-TiO_2 prepared in FB

Together, these effects produce higher microscopic and macroscopic displacement efficiencies under core conditions [21,51]. Incremental recoveries of this magnitude (double-digit OOIP for tertiary surfactant floods) are consistent with reported laboratory EOR studies using natural saponins and nanoparticle-assisted floods when the rock is initially oil-wet and the formulation is tailored to reservoir salinity/temperature. The hybrid approach often yields higher incremental recovery than surfactant alone, as seen in the reported literature and reproduced here. The superior performance of the hybrid flood suggests that field-scale pilots should consider nanoparticle inclusion where economics, injectivity, and formation sensitivity permit. Nonetheless, several operational concerns must be addressed before field rollout: nanoparticle retention in the formation, long-term stability under reservoir geochemistry, scale-up of extraction/purification of chickweed surfactant to supply required volumes, and economic analysis versus synthetic alternatives. The core results provide a strong technical basis for proceeding to 1D/3D flow simulations and scaled pilot tests, with attention to optimizing nanoparticle concentration and surfactant dosing aligned to formation brine chemistry [35,51,52].

4. Conclusions

In conclusion, the experimental results demonstrate the significant impact of various solutions on crude oil recovery under reservoir conditions. Interfacial tension measurements indicated that the addition of natural surfactants and salts effectively reduced IFT, facilitating improved oil mobilization. Contact angle analyses revealed that these solutions could alter rock wettability from oil-wet toward more water-wet conditions over time, with the extent of wettability change correlating with the soaking duration. Core flooding experiments further confirmed these findings, showing that secondary recovery using formation brine was limited, whereas tertiary recovery with smart surfactant-based solutions substantially enhanced oil recovery. Notably, the combination of surfactant with different salinity solutions influenced both the recovery efficiency and the optimal soaking period. Overall, the study highlights the critical role of tailored chemical formulations and wettability alteration in maximizing oil recovery, providing valuable insights for designing enhanced oil recovery strategies under reservoir-relevant conditions. The findings of this work provide a clear pathway for translating the chickweed-derived surfactant and its hybrid formulation with Nano-TiO_2 into practical EOR applications. The strong IFT reduction, notable wettability alteration toward water-wet conditions, and the enhanced tertiary recovery observed in carbonate cores indicate that this natural surfactant system can serve as a viable alternative to conventional chemical agents, particularly in high-salinity and elevated-temperature reservoirs where synthetic surfactants often fail. Because chickweed is inexpensive, widely accessible, and easily processed, its large-scale extraction can be integrated into existing chemical supply chains with minimal environmental burden. Future studies should focus on pilot-scale flooding tests, long-term adsorption and retention behavior in reservoir rocks, and the optimization of surfactant–nanoparticle ratios for field deployment. Moreover, evaluating the economic feasibility and assessing potential environmental impacts under real reservoir conditions will be important steps toward full-scale implementation. These directions will help bridge the gap between laboratory performance and operational EOR strategies, bringing sustainable surfactant technology closer to field application.

Acknowledge

The authors gratefully acknowledge and appreciate the Department of Petroleum Engineering, Faculty of Engineering, Marvdasht Islamic Azad University, Marvdasht, Iran and to Fars EOR Technologies Company, for the provision of the laboratory facilities necessary for completing this work.

Authors Contribution
All the authors have participated sufficiently in the intellectual content, conception and design of this work or the analysis and interpretation of the data (when applicable), as well as the writing of the manuscript.

Availability of data and materials
The data that support the findings of this study are available from the corresponding author, upon reasonable request.

Conflict of interests
The author states that there is no conflict of interest.

References

[1] Gandomkar A, Kharrat R. Anionic surfactant adsorption through porous media in carbonate cores: An experimental study. Energy Sources A Recover Util Environ Eff. 2013; 35:58-65. https://doi.org/10.1080/15567036.2010.501368

[2] Gandomkar A, Kharrat R, Motealleh M, Khanamiri HH, Nematzadeh M, Ghazanfari MH. An experimental investigation of foam for gas mobility control in a low-temperature fractured carbonate reservoir. Pet Sci Technol. 2012; 30:976-985. https://doi.org/10.1080/10916466.2010.493905

[3] Motealleh M, Kharrat R, Gandomkar A, Khanamiri H, Nematzadeh M, Ghazanfari M. An experimental study on the applicability of water-alternating-CO2 injection in the secondary and tertiary recovery in one Iranian reservoir. Pet Sci Technol. 2012; 30:2571-2581. https://doi.org/10.1080/10916466.2010.514584

[4] Nematzadeh M, Khanamiri H, Aghajani M, Kharrat R, Gandomkar A, Motealleh M, et al. An experimental study of secondary WAG injection in a low-temperature carbonate reservoir in different miscibility conditions. Pet Sci Technol. 2012; 30:1359-1368. https://doi.org/10.1080/10916466.2010.504935

[5] Sharma G, Dwivedi K, Bafana A, Pakade Y, OICC RB. Wet air oxidation of leachate containing emulsified and solubilized hydrocarbons from crude oil-contaminated soil. Int J Ind Chem. 2023;10. https://doi.org/10.1007/s40090-019-0187-2

[6] Quintella CM, Rodrigues PD, Ramos-de-Souza E, Carvalho EB, Nicoleti JL, Hanna SA. Integration of EOR/IOR and environmental technologies in BRICS and nonBRICS: A patent-based critical review. Energy Rep. 2025; 13:747-758. https://doi.org/10.1016/j.egyr.2024.11.081

[7] Ramesh Dadi N, Kumar Maurya N, Gupta P. Advancing foam EOR: A comprehensive examination of key parameters and mechanisms from surfactants to nanoparticles. J Mol Liq. 2024; 415:126177. https://doi.org/10.1016/j.molliq.2024.126177

[8] Bello MN, Shafiei A. A novel green nanocomposite for EOR: Experimental investigation of IFT reduction, wettability shift, and nanofluid stability. J Mol Liq. 2024; 414:126187. https://doi.org/10.1016/j.molliq.2024.126187

[9] Rajan KP, Gopanna A, Theravalappil R, Thomas SP. Systematic design, implementation and students' perceptions of a polymer engineering course for chemical engineering curricula. Int J Ind Chem. 2024;15. https://doi.org/10.57647/j.ijic.2024.1501.04

[10] Jianga J, Du J, Ren C, Liu Y, Gao X, Li L. Research on the influencing factors of estimated ultimate recovery after shale gas well fracturing. Int J Ind Chem. 2024;15. https://doi.org/10.57647/j.ijic.2024.1502.09

[11] Gandomkar A, Kharrat R. The tertiary FAWAG process on gas and water invaded zones: An experimental study. Energy Sources A Recover Util Environ Eff. 2012; 34:1913-1922. https://doi.org/10.1080/15567036.2010.493921

[12] Gandomkar A, Torabi F, Enick RM. Enhanced oil recovery via dissolution of low molecular weight PDMS in CO2 during immiscible gas injection in matrix-fracture system. Chem Eng Res Des. 2024; 203:18-28. https://doi.org/10.1016/j.cherd.2024.01.022

[13] Kumar Pandey R, Gandomkar A, Vaferi B, Kumar A, Torabi F. Supervised deep learning-based paradigm to screen the enhanced oil recovery scenarios. Sci Rep. 2023; 13:4892. https://doi.org/10.1038/s41598-023-32187-2

[14] Gandomkar A, Torabi F, Nasriani HR, Enick RM. Decreasing asphaltene precipitation and deposition during immiscible gas injection via the introduction of a CO2-soluble asphaltene inhibitor. SPE J. 2023; 28:2316-2328. https://doi.org/10.2118/214698-PA

[15] Sami B, Azdarpour A, Honarvar B, Nabipour M, Keshavarz A. Application of a novel natural surfactant extracted from Avena sativa for enhanced oil recovery during low salinity water flooding: Synergism of natural surfactant with different salts. J Mol Liq. 2022; 362:119693. https://doi.org/10.1016/j.molliq.2022.119693

[16] Soapnut extract as a natural surfactant for enhanced oil recovery. Energy Sources A Recover Util Environ Eff. 2009;31(20). https://doi.org/10.1080/15567030802462622

[17] Navaie F, Esmaeilnezhad E, Jin Choi H. Xanthan gum-added natural surfactant solution of Chuback: A green and clean technique for enhanced oil recovery. J Mol Liq. 2022; 354:118909. https://doi.org/10.1016/j.molliq.2022.118909

[18] Norouzpour M, Nabipour M, Azdarpour A, Akhondzadeh H, Santos RM, Keshavarz A. Experimental investigation of the effect of a quinoa-derived saponin-based green natural surfactant on enhanced oil recovery. Fuel. 2022; 318:123652. https://doi.org/10.1016/j.fuel.2022.123652

[19] Moradi M, Karimi S, Behnajady B, Esmailzadeh M. Green solvent-driven chalcopyrite dissolution: Ternary DES (ChCl/MOA/PTSA) for high-efficiency copper extraction via RSM optimization, kinetics, and molecular dynamics insights. Miner Eng. 2025; 233:109606. https://doi.org/10.1016/j.mineng.2025.109606

[20] Azdarpour A, Mohammadian E, Norouzpour M, Liu B. The effects of a novel bio-based surfactant derived from the Acacia concinna plant on chemical enhanced oil recovery in the presence of various salts and a synthesized HSPAM polymer. J Mol Liq. 2023; 386:122474. https://doi.org/10.1016/j.molliq.2023.122474

[21] Cerón-Camacho R, Cisneros-Dévora R, Soto-Castruita E, Ramírez-Pérez JF, Martínez-Magadán JM, Oviedo-Roa R, et al. Greener process to prepare and scale-up zwitterionic macro cyclic dihydroxy-aza-crown ether and their corresponding supramolecular pairs to enhanced oil recovery application. J Clean Prod. 2023; 420:138446. https://doi.org/10.1016/j.jclepro.2023.138446

[22] Torabi F, Gandomkar A. Experimental evaluation of CO2-soluble nonionic surfactants for wettability alteration to intermediate CO2-oil wet during immiscible gas injection. SPE J. 2024; 29:5071-5086.

https://doi.org/10.2118/221487-PA

[23] Abou-Alfitooh SAM, El-Hosiny FI, El-Hoshoudy AN. Experimental and computational study of modified biopolymer xanthan gum with synthetic vinyl monomers for enhanced oil recovery. J Polym Environ. 2024; 32:6256-6275. https://doi.org/10.1007/s10924-024-03346-x

[24] Manshad AK, Mobaraki M, Ali JA, Akbari M, Abdulrahman AF, Jaf PT, et al. Performance evaluation of the green surfactant-treated nanofluid in enhanced oil recovery: Dill-hop extracts and SiO2/bentonite nanocomposites. Energy Fuels. 2024; 38:1799-1812. https://doi.org/10.1038/s41598-024-53055-7

[25] Mehrabianfar P, Momeni M, Razzaghi-Koolaee F, Eslahati M, Malmir P, Soltani Soulgani B. Introduction of a novel mathematical model for the prediction of the preformed particle gel's swelling in the presence of monovalent and divalent ions. Sci Rep. 2024; 14:3243. https://doi.org/10.1038/s41598-024-53055-7

[26] Mehrabianfar P, Malmir P, Soltani Soulgani BS, Hashemi A. Study on the optimization of the performance of preformed particle gel (PPG) on the isolation of high permeable zone. J Pet Sci Eng. 2020; 195:107530. https://doi.org/10.1016/j.petrol.2020.107530

[27] Eslahati M, Mehrabianfar P, Isari AA, Bahraminejad H, Manshad AK, Keshavarz A. Experimental investigation of alfalfa natural surfactant and synergistic effects of Ca2+, Mg2+, and SO4 2− ions for EOR applications: Interfacial tension optimization, wettability alteration and imbibition studies. J Mol Liq. 2020; 310:113123. https://doi.org/10.1016/j.molliq.2020.113123

[28] Mehrabianfar P, Bahraminejad H, Manshad AK. An introductory investigation of a polymeric surfactant from a new natural source in chemical enhanced oil recovery (CEOR). J Pet Sci Eng. 2021; 198:108172. https://doi.org/10.1016/j.petrol.2020.108172

[29] Razzaghi-Koolaee F, Mehrabianfar P, Soltani Soulgani B, Esfandiarian A. A comprehensive study on the application of a natural plant-based surfactant as a chemical enhanced oil recovery (CEOR) agent in the presence of different ions in carbonate reservoirs. J Environ Chem Eng. 2022; 10:108572. https://doi.org/10.1016/j.jece.2022.108572

[30] Gandomkar A, Honarvar B, Kazemzadeh Y, Derikvand Z. An experimental study of surfactant alternating CO2 injection for enhanced oil recovery of carbonated reservoir. Iran J Oil Gas Sci Technol. 2016; 5:1-17. https://doi.org/10.22050/ijogst.2016.41564

[31] Bashti N, Gandomkar A, Sharif M. The effect of P-1-D thickener on CO2 mobility control during enhanced oil recovery. J Pet Res. 2020; 30:103-112. https://doi.org/10.22078/pr.2020.3944.2798

[32] Nowrouzi I, Mohammadi AH, Manshad AK. Characterization and evaluation of a natural surfactant extracted from soapwort plant for alkali-surfactant-polymer (ASP) slug injection into sandstone oil reservoirs. J Mol Liq. 2020; 318:114369. https://doi.org/10.1016/j.molliq.2020.114369

[33] Dashtaki SRM, Ali JA, Majeed B, Manshad AK, Nowrouzi I, Iglauer S, et al. Evaluation the role of natural surfactants from Tanacetum and tarragon plants in EOR applications. J Mol Liq. 2022; 361:119576. https://doi.org/10.1016/j.molliq.2022.119576

[34] Amamra S, Kaabi I, Arrar L, Baghiani A, Hamla M, Aouni SI, et al. Thymus vulgaris extract: A green approach to antioxidant efficacy, antibacterial action, and corrosion inhibition. J Environ Chem Eng. 2025; 13:116067. https://doi.org/10.1016/j.jece.2025.116067

[35] Singh A, Sharma T, Kumar RS, Arif M. Biosurfactant derived from fenugreek seeds and its impact on wettability alteration, oil recovery, and effluent treatment of a rock system of mixed composition. Energy Fuels. 2023; 37:6683-6696. https://doi.org/10.1021/acs.energyfuels.3c00105

[36] Viveros LTL, Rafati R, Sharifi Haddad A. Impact of coated and non-coated magnetic nanoparticles on oil-water separation in green surfactant-based emulsions. Colloids Surf A Physicochem Eng Asp. 2024; 697:134366. https://doi.org/10.1016/j.colsurfa.2024.134366

[37] Kamari A, Pournik M, Rostami A, Amirlatifi A, Mohammadi AH. Characterizing the CO2-brine interfacial tension (IFT) using robust modeling approaches: A comparative study. J Mol Liq. 2017; 246:32-38. https://doi.org/10.1016/j.molliq.2017.09.010

[38] Nowrouzi I, Mohammadi AH, Manshad AK. Water-oil interfacial tension (IFT) reduction and wettability alteration in surfactant flooding process using extracted saponin from Anabasis setifera plant. J Pet Sci Eng. 2020; 189:106901. https://doi.org/10.1016/j.petrol.2019.106901

[39] Deljooei M, Zargar G, Nooripoor V, Takassi MA, Esfandiarian A. Novel green surfactant made from L-aspartic acid as enhancer of oil production from sandstone reservoirs: Wettability, IFT, microfluidic, and core flooding assessments. J Mol Liq. 2021; 323:115037. https://doi.org/10.1016/j.molliq.2020.115037

[40] Nafisifar A, Khaksar Manshad A, Reza Shadizadeh S. Evaluation of a new green synthesized surfactant from linseeds: Chemical EOR implications from sandstone petroleum reservoirs. J Mol Liq. 2021; 342:117263. https://doi.org/10.1016/j.molliq.2021.117263

[41] Asl FO, Zargar G, Manshad AK, Iglauer S, Keshavarz A. Experimental investigation and simulation for hybrid of nanocomposite and surfactant as EOR process in carbonate oil reservoirs. Fuel. 2022; 319:123591. https://doi.org/10.1016/j.fuel.2022.123591

[42] Ahmadi P, Asaadian H, Khadivi A, Kord S. A new approach for determination of carbonate rock electrostatic double layer variation towards wettability alteration. J Mol Liq. 2019; 275:682-698. https://doi.org/10.1016/j.molliq.2018.11.106

[43] Bachu S, Bennion DB. Interfacial tension between CO2, freshwater, and brine in the range of pressure from (2 to 27) MPa, temperature from (20 to 125) °C, and water salinity from (0 to 334000) mg·L−1. J Chem Eng Data. 2009; 54:765-775. https://doi.org/10.1021/je800529x

[44] Jacob R, Saylor BZ. CO2 solubility in multi-component brines containing NaCl, KCl, CaCl2 and MgCl2 at 297 K and 1–14 MPa. Chem Geol. 2016; 424:86-95. https://doi.org/10.1016/j.chemgeo.2016.01.013

[45] Hejri Z, Hejri M, Omidvar M, Morshedi S. Synthesis of TiO2/nZVI nanocomposite for nitrate removal from aqueous solution. Int J Ind Chem. 2019;10. https://doi.org/10.1007/s40090-019-0186-3

[46] Aminian A, ZareNezhad B. Wettability alteration in carbonate and sandstone rocks due to low salinity surfactant flooding. J Mol Liq. 2019; 275:265-280. https://doi.org/10.1016/j.molliq.2018.11.080

[47] Amin JS, Nikooee E, Ghatee MH, Ayatollahi S, Alamdari A, Sedghamiz T. Investigating the effect of different asphaltene structures on surface topography and wettability alteration. Appl Surf Sci. 2011; 257:8341-8349. https://doi.org/10.1016/j.apsusc.2011.03.123

[48] Khani M, Pordel M, Davoodnia A, TavasoliFarsheh A. Investigation of the effect of using ZnO/TiO2 nanoparticles on properties of the polyethylene terephthalate preform and beverage bottles. Int J Ind Chem. 2022;13. Available from: https://oiccpress.com/ijic/article/view/8246 (accessed October 29, 2025).

[49] Liu S, Geng Y, Li C, Hu M, Liu J, Gao Q, et al. Exploring the microscopic synergism of hydrophobic nanoparticles and surfactants in surfactants-assisted nanofluids (SAN) for enhanced oil recovery. Geoenergy Sci Eng. 2025; 246:213632. https://doi.org/10.1016/j.geoen.2024.213632

[50] Panagopoulos D, Alamdari AA, Quinson J. Surfactant-free colloidal gold nanoparticles: Room temperature synthesis, size control and opportunities for catalysis. Mater Today Nano. 2025; 29:100600. https://doi.org/10.1016/j.mtnano.2025.100600

[51] Al-Ghamdi A, Haq B, Al-Shehri D, Muhammed NS, Mahmoud M. Surfactant formulation for green enhanced oil recovery. Energy Rep. 2022; 8:7800-7813. shttps://doi.org/10.1016/j.egyr.2022.05.293

[52] El-Masry JF, Maalouf E, Abbas AH, Bou-Hamdan KF. Advancements in green materials for chemical enhanced oil recovery: A review. Petroleum. 2025; 11:259-276. https://doi.org/10.1016/j.petlm.2025.03.007